Postadsorption Rearrangements of Block Copolymer Micelles at the Solid/Liquid Interface

Ryan Toomey,[†,⊥] Jimmy Mays,[‡,§] Jinchuan Yang,[‡] and Matthew Tirrell*[,†]

Department of Chemical Engineering and Materials Research Laboratory, University of California at Santa Barbara, Santa Barbara, California 93106; Department of Chemistry, University of Tennessee, Knoxville, Tennessee 37996; and Chemical Sciences Division, Oak Ridge National Laboratory, Oak Ridge, Tennessee 37831

Received May 27, 2005; Revised Manuscript Received December 10, 2005

ABSTRACT: The influence of postadsorption relaxation processes has been evaluated in the adsorption behavior of block copolymer micelles comprised of asymmetric poly(*tert*-butylstyrene-*b*-sodium 4-styrenesulfonate) (PtBS−NaPSS) diblock copolymers as well as star-block copolymers of similar size and composition. The adsorptions were conducted from aqueous solutions to an uncharged, hydrophobic octadecyltrichlorosilane (OTS) surface, which is highly selective for the hydrophobic PtBS block. The star-block copolymer adsorption kinetics scale linearly with concentration over the entire adsorption process and follow behavior characteristic of random sequential adsorption (RSA). At long times, the star-blocks approach a jamming limit with $t^{-1/2}$ kinetics. The micelles, in contrast, show no sign of a jamming limit and adsorb according to log(t) kinetics, signifying that the adsorbed layer is able to relax during the adsorption process. Furthermore, the rate of adsorption of the micelles scales nonlinearly with concentration at long times, indicating that the time scale of this relaxation is on the same order of magnitude as the characteristic adsorption time.

I. Introduction

Amphiphilic block copolymers have garnered extensive experimental[1−10] and theoretical[11−19] interest as they have the capacity to self-organize at the liquid−solid interface. Structural control is engendered through insoluble "anchor" blocks, which facilitate surface assembly by preferentially adsorbing over the soluble "buoy" segments in the block copolymer.[15] For instance, attaching the anchor block to the end of a soluble block renders a so-called "brush" adsorbed layer, where the soluble chains protrude from the surface tethered through the anchor block. This copolymer architecture minimizes loop formation and produces the thickest layers. The particular sequence and relative sizes of the blocks can be chosen to finely tune the overall structure, making block copolymers powerful candidates for the control and manipulation of surface properties.

An unresolved question involving block copolymer adsorption, however, is the effectiveness to which a copolymer can be designed and the adsorption carried out "to order". For instance, the manner in which a polymer chain initially populates a solid surface may involve strong departure from an equilibrium conformation.[20] The success to which the thermodynamically stable structure can be adopted depends on the ease to which the adsorbed polymers can diffuse and reconfigure. In the very least, such surface processes would be expected to influence the adsorption kinetics, especially if both activities occur on similar time scales.[21−23]

Similar to homopolymers and proteins, block copolymers can display complicated adsorption patterns; however, the adsorption of block copolymers has potentially richer behavior due to self-association aspects. In selective solvents, the anchor blocks create higher-order structures, such as micelles. The precise role that these structures play is fundamentally important as the characteristic time scales for adsorption and layer assembly are affected by their presence. Nonetheless, the role that these structures play remains unclear. In the case that micelles adsorb, development of the thermodynamically stable brush structure will depend on the rate to which adsorbed micelles can relax and reorganize at the surface. The surface micelles may be capable of spreading, dissociation, or fusion. It is expected that the adsorption rate in this stage depends not only on the number of preadsorbed species but also on the conformation of those species. Therefore, the adsorption probability in this regime may be a function of both the adsorbed amount and time. The "brush" structure emerges when the anchor blocks reach sufficient density to displace adsorbed coronal chains. The immediate consequence of such behavior is that the adsorption kinetics may be controlled to a larger degree by transient states rather than equilibrium conditions.

In this work, we investigate the adsorption behavior of diblock copolymer poly(*tert*-butyl styrene)-*b*-poly(sodium 4-styrenesulfonate) (PtBS−NaPSS) micelles and similarly sized PtBS−NaPSS star-block copolymers to address the role and time scale of post-adsorption rearrangements on the interfacial assembly of brush layers from micellar solutions. The star-block copolymer mimics the micellar structure but cannot undergo dissociation, allowing direct comparison of the adsorption kinetics. All adsorptions are carried out with hydrophobic OTS surfaces, which are highly selective for the PtBS block, and monitored in situ with phase-modulated ellipsometry.

II. Materials and Methods

Materials. Diblock and star-block copolymers of PtBS and NaPSS were produced by selective sulfonation of precursor block PtBS and polystyrene (PS) copolymers. All block copolymers were synthesized by sequential anionic polymerization as previously described. [24] The polymers were sulfonated by the method of Valint and Bock to yield ∼90% sulfonation for all samples.[25] The sulfonic

[†] University of California at Santa Barbara.
[‡] University of Tennessee.
[§] Oak Ridge National Laboratory.
[⊥] Current address: Department of Chemical Engineering, University of South Florida, Tampa, FL 33620.
* Corresponding author. E-mail: tirrell@engineering.ucsb.edu.

10.1021/ma051097i CCC: $33.50
Published on Web 02/25/2006

Table 1. Polymer Molecular Characteristics

sample	M_w NaPSS	M_w PtBS	M_w/M_n	sulfonation (%)[a]	f[b]	N_{NaPSS}[c]	N_{PtBS}[c]
$NaPSS_{444}$	87 000		1.1	90		444	
$PtBS_{15}$-*b*-$NaPSS_{438}$	86 000	2400	1.05	90		438	15
$PtBS_{10}$-*star*-$NaPSS_{307}$	62 500	1650	1.12	95	10	307	10

[a] Sulfonation degree is calculated from the elemental analysis analysis data on sulfur. [b] Star functionality based on weight-average number of arms. [c] Weight-average degree of polymerization.

acid groups were neutralized using sodium methoxide to generate the final block copolymers. To preserve their water solubility, all the copolymers were made highly asymmetric with a small hydrophobic PtBS block relative to a large NaPSS block. NaPSS homopolymer of molecular weight 87 000 was purchased from Polysciences and used as received. The molecular characteristics of the polymers are shown in Table 1. Optically clear solutions were obtained by dissolving the polymer in Milli-Q water at a known concentration (100−500 ppm) and stirring for 2−4 weeks. At ∼1 week prior to the experiment, the solutions were diluted to the desired concentration and the appropriate amount of sodium chloride was added. At this time, the solutions were gently stirred at 90 °C for 3 days followed by 4 days at room temperature to ensure equilibrium and reproducibility of the solution. Immediately before the experiment, the solutions were filtered through a 0.45 μm polycarbonate filter.

Silicon surfaces for adsorption were prepared in the following way. (100)-oriented, double-sided polished, test grade silicon wafers (Virginia Semiconductor) were cut into pieces of appropriate size (∼1 cm^2) and cleaned by a two-step process. First, they were dipped into a freshly made 70:30 (v/v) sulfuric acid/hydrogen peroxide solution for 10−15 min followed by rinsing under Milli-Q water for 3−5 min. To remove any remaining contaminants, the wafers were exposed to a UV cleaning chamber between 5 and 10 min. The UV light source was a low-pressure mercury quartz lamp. This treatment yields a hydrophilic, contaminate-free surface with a native oxide (SiO_2) layer of 14−15 Å thick, as checked by ellipsometry. Water will completely wet the surface. If there was a finite contact angle with water, the cleaning process was repeated. These cleaned surfaces were used within 10 min of preparation.

To prepare the hydrophobic surfaces, octadecylsilane (OTS) films were made by immersing the substrates in 10^{-3} mol/L solutions of octadecyltrichlorosilane in toluene for 1−2 h. Octadecyltrichlorosilane (Aldrich, 95%) and toluene (Sigma-Aldrich, HPLC grade, 99.8%) were commercially available and used as received. The coating solutions were used for no more than 1−2 days, after which they were discarded and new solutions made. The film-covered substrates were then removed from the solution and baked at 110 °C for 1 h to remove any excess water and drive complete hydrolysis of the OTS layer. If the OTS deposition was successful, the toluene solution dewets the surface and beads off as the substrate is removed. Following the baking step, the substrates were sonicated in HPLC grade chloroform to remove any loose OTS.

Ellipsometry showed the final film thickness was on the order of 20−22 Å (the contour length of a single molecule is 26 Å); therefore, the surface coverage is on the order of 80%. Typical advancing angles were 110°−115° and receding angles were 100°−105°. Receding angles of less than 95° indicated a poorly formed layer, and these substrates were discarded.

Ellipsometry Measurements. All adsorption experiments were conducted with a Beaglehole picometer ellipsometer, which uses a He−Ne laser light source ($\lambda = 632.8$ nm), has an angular resolution of 1/100, and is based on the phase modulation technique of Jasperson and Schnatterley.[26] The ellipsometer directly measures the real and imaginary components of the ellipsometric ratio[27]

$$\rho = \frac{r_p}{r_s} = \tan \Psi e^{i\Delta} \qquad (1)$$

where $\mathrm{Re}(\rho) = \tan \Psi \cos \Delta$ and $\mathrm{Im}(\rho) = \tan \Psi \sin \Delta$. r_p and r_s are the complex overall reflection coefficients of the p and s polarizations, respectively. The angles Ψ and Δ correspond to the ratio of attenuation of the p and s polarizations and the phase change between the p and s polarizations, respectively.

At the beginning of the experiment, either a freshly cleaned silicon substrate or OTS/silicon substrate was inserted into a specially built cylindrical solution cell. The cell was then filled with polymer-free solution at the desired salt concentration. The angle of incidence was set at the Brewster angle (∼71°) for the water/silicon interface. At this angle, $\Delta = 90°$ and $\mathrm{Im}(\rho) \leq 0.005$. If $\mathrm{Im}(\rho)$ remained constant over the next 15 min, the polymer solution was introduced through the cell inlet. The adsorbed amount (mass/area) was then determined using the following analysis[28]

$$\mathrm{Im}(\rho) - \mathrm{Im}(\rho)_{\mathrm{baseline}} = \frac{2\pi}{\lambda} \frac{\sqrt{n_{\mathrm{solvent}}^2 + n_{\mathrm{substrate}}^2}}{n_{\mathrm{solvent}}} \left(\frac{dn}{dc}\right) \Gamma \qquad (2)$$

where $\lambda = 632.8$ nm, $n_{\mathrm{solvent}} = 1.33$, $n_{\mathrm{substrate}} = 3.88$, and $dn/dc = 0.168$ mL/g.[29]

III. Results and Discussion

In a previous publication,[30] the adsorption kinetics of $PtBS_{15}$-*b*-$NaPSS_{438}$ micelles suggest that they directly adsorb from a stagnant solution to hydrophobic surfaces, albeit at a rate slower than the solution diffusion rates would suggest, by at least an order of magnitude. The soluble corona of the micelle provides a "repelling" layer and thus creates an energy barrier for adsorption. This lead us to the thinking that, to a barren surface, the micelles have a certain sticking probability based on the number of corona-surface contacts made during a surface collision at the expense of coronal deformation. To fully understand the adsorption behavior of the micelles, two questions emerge: (1) during the adsorption event, is the micelle able to relax and adopt a structure wherein the core blocks find the surface, and (2) does this relaxation lead to a spreading of the micelle or a molecular rearrangement that can be inferred from the adsorption kinetics? Because the time scale of postadsorption relaxation events should be correlated to the size and the glass transition temperature of the core blocks, block copolymers with short PtBS blocks (15) were studied. The behavior is subsequently compared to star-block copolymers of similar size and composition to the micelles.

To answer the first question, whether a micelle has the capacity to relax during the adsorption event, Figure 1 illustrates the adsorption of $PtBS_{15}-NaPSS_{438}$ micelles to a surface that has been previously saturated with $NaPSS_{444}$ homopolymer. The experiment first involves the adsorption of $NaPSS_{444}$ to an OTS surface. As the surface coverage nears 1 mg/m^2, it appears that adsorption is almost complete (in actuality it is still increasing, but with the logarithm of time). At this point, the $NaPSS_{444}$ homopolymer is replaced by $PtBS_{15}-NaPSS_{438}$ micelles at the same adsorbing concentration. Almost immediately, the surface coverage increases. In fact, a comparison of micelle adsorption to the preadsorbed NaPSS layer with that to the barren OTS surface indicates a very similar adsorption initial adsorption rate (ca. 0.003 $mg/(m^2\ s)$), suggesting that preadsorbed NaPSS shows negligible resistance to micelle adsorption. While it could be argued that the NaPSS coronal chains of the micelle are exchanging with the adsorbed NaPSS homopolymer, prior

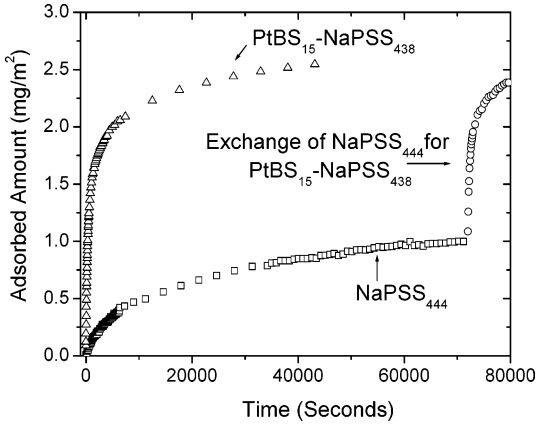

Figure 1. Adsorption of $PtBS_{15}-NaPSS_{438}$ micelles (○) to a pre-adsorbed $NaPSS_{444}$ (□) layer on OTS. For comparison, the adsorption of the micelles to the barren OTS surface is also shown (△). All polymer concentrations are 100 ppm, and NaCl concentration is 0.3 M.

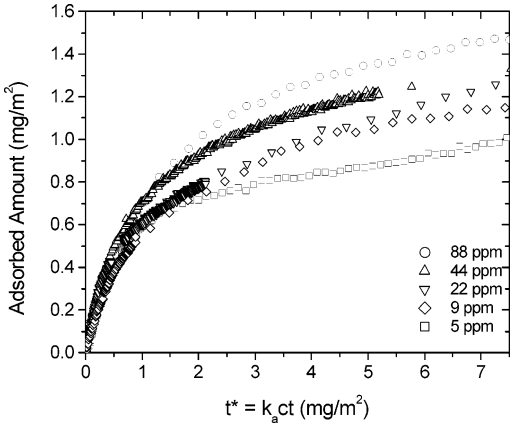

Figure 2. Adsorption of $PtBS_{15}-NaPSS_{438}$ to OTS at 0.3 M NaCl as a function of the rescaled time $k_a ct$.

investigations have demonstrated that exchange between like species tends to be quite slow.[31] On the other hand, when the selectivity of the surface is orders of magnitude in favor of the second species, the latter will adsorb at a rate approaching its adsorption rate to a barren surface.[31] Therefore, it could be interpreted that the coronal arms of the micelle must reconfigure relatively quickly after adsorption, permitting the PtBS blocks to stabilize the adsorbed species. Without this relaxation mechanism, it is unlikely that the micelles would adsorb as quickly to a surface coated with a mature NaPSS layer.

To further explore the consequences of adsorption-induced rearrangements or relaxation events associated with the adsorbed micelles, Figure 2 shows the rate of layer growth of the $PtBS_{15}-NaPSS_{438}$ micelles over a range of adsorbing concentrations. To aid in the interpretation of the data, the adsorbed amount Γ is plotted against the rescaled time $t^* = k_a ct$, where k_a is the apparent adsorption rate constant, c is the bulk concentration, and t is time. The rate constant k_a is determined from the maximum rate of adsorption J_0 measured in the start of the experiment. The adsorbing concentration was varied between 5 and 88 ppm, and these concentrations were chosen as they provided adsorption rates that could be reliably measured in the initial stages of adsorption. In such a plot, the initial slope is unity, which signifies that bulk transfer from solution to the surface controls layer growth. As the surface becomes progressively more crowded, however, the growth rate is retarded as a result of interferences from the growing layer, and the slope deviates from unity. As the available binding sites disappear,

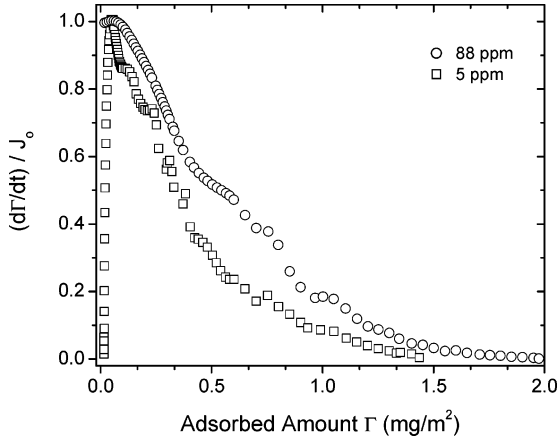

Figure 3. Normalized adsorption rate of $PtBS_{15}-NaPSS_{438}$ to OTS at 0.3 M NaCl as a function the adsorbed amount for solution concentrations of 88 ppm (○) and 5 ppm (□).

the adsorption slope continually transitions to zero at saturation, the rate of which provides important clues as to how the layer is formed. The adsorbed amount will be a unique function of $k_a ct$ up until a time when significant surface structural changes occur. Three events that could possibly occur after micelle adsorption include (1) relaxation of the individual coronal arms to form loops, trains, and tails, (2) self-diffusion of the entire micelle, and (3) spreading or dissociation of the adsorbed micelle.

In Figure 2, while the adsorbed amount Γ is initially described by the rescaled time $k_a ct$, the adsorption curves diverge at higher surface coverages and follow different kinetic trajectories. For instance, in comparing the 88 and 5 ppm trajectories, the two curves deviate at ~0.3 mg/m^2 and the slope of the 88 ppm case remains greater throughout the entire adsorption process. In other words, higher micelle concentrations lead to higher adsorbed amounts under otherwise equivalent conditions.

While the kinetic regimes can be inferred from the Γ vs $k_a ct$ plots, their identification can be facilitated by plotting the adsorption rate $d\Gamma/dt$ vs the adsorbed amount Γ.[32] The derivation, nevertheless, amplifies noise in the experimental data, which were collected at 1 s intervals. Consequently, the derivative curves were smoothed using cubic-spline interpolation and 10-point averaging. The resulting time derivatives were then normalized with the initial rate J_0 and are shown in Figure 3 for the 5 and 88 ppm cases. The initial rise in the adsorption rate, seen in both curves, corresponds to a brief induction period as the sample is injected into the adsorption cell. In the 88 ppm case, the maximum adsorption rate is maintained up to 0.2 mg/m^2, followed by a sharp decrease, corresponding to an increasing barrier to adsorption. In the 5 ppm case, not only does the attenuation of the adsorption rate start at a lower surface coverage (0.1 mg/m^2), but the adsorption rate also falls at a faster rate. At an adsorbed amount of 1 mg/m^2, the rate has fallen to 10% of its initial value at 5 ppm but only to 20% in the 88 ppm case.

Of the three events that could occur after a micelle adsorbs, the effect of translational mobility or self-diffusion of the micelles would produce the opposite trend in the experimental data, favoring higher surface coverage for lower bulk concentrations.[22] The reason can be understood by the following argument. If the characteristic adsorption time is short (corresponding to a high bulk concentration), the adsorbed particles will not migrate significantly on the surface before the arrival of new micelles. On the other hand, if insertions occur less often, then the adsorbed particles have more time to diffuse, and the

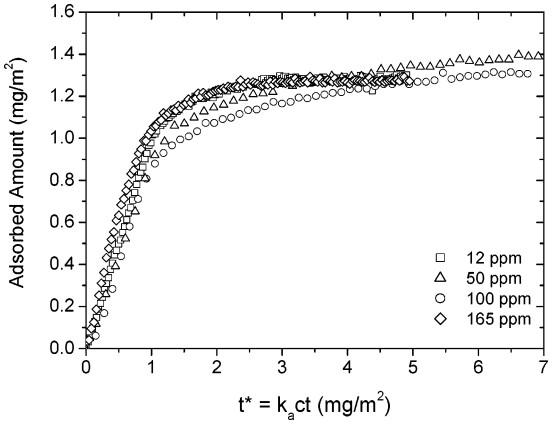

Figure 4. Adsorption of $PtBS_{10}$-star-$NaPSS_{307}$ to OTS at 0.3 M NaCl as a function of rescaled time $k_a ct$.

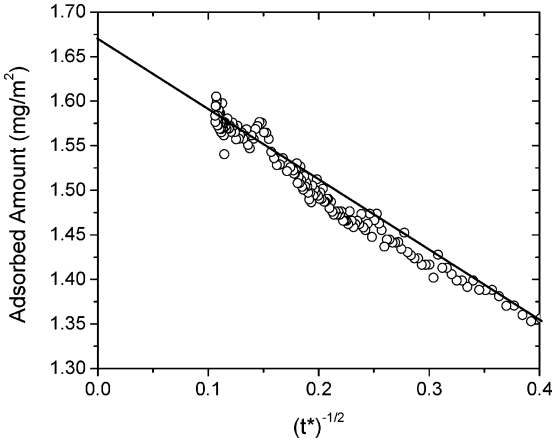

Figure 5. Late coverage adsorption of $PtBS_{10}$-star-$NaPSS_{307}$ to OTS at 0.3 M NaCl and a concentration of 100 ppm as a function of $t^{-1/2}$. In a pure RSA process, the intercept signifies the surface coverage at the jamming limit, and the data will approach the intercept as $t^{-1/2}$.

adsorbed layer can relax to a more efficiently packed configuration, which favors higher adsorbed amounts. The two other scenarios include relaxation of the individual arms and a spreading of the adsorbed micelle. The unfolding of flexible homopolymers is thought to occur on time scales of less than a second, so it is doubtful this would show up in the experimental window.[33] Therefore, the data suggest that immediately after adsorbing the micelles somehow spread and effectively compete for available surface space with newly arriving micelles, analogous to how proteins denature at surfaces and unfold.[21,34−36] At lower polymer concentrations, the adsorbed micelles have more time to spread and fill empty space. As a consequence of this spreading, incoming micelles are more likely to feel the presence of the adsorbed layer and thus adsorption slows. This idea is supported by the theoretical work of Liguoure, who showed that if the spreading power of the anchor block is sufficiently strong (where the contact angle is less than a critical value of 51°), a surface micelle will have a lower equilibrium aggregation number than the bulk micelle.[37] For blocks that completely wet the surface, surface aggregation is unstable, and adsorbed micelles will eventually lead to a uniform layer, provided the chains can diffuse laterally on the surface.

The estimated average aggregation number of a micelle is on the order of 10, and the hydrodynamic radius is 220 Å.[30] On the basis of these numbers, the approximate surface coverage of a closely packed monolayer of micelles is 1.4 mg/m^2. Consequently, the approximate time to reach the overlap surface coverage $\tau_a = \Gamma_{max}/J_0$ is 300 s for the 88 ppm case (the initial adsorption rate is 0.005 mg/(m^2 s)) case and 1 h for the 5 ppm cases. To be observed in the experimental window, therefore, the micelles must spread on a time scale of minutes, which also is consistent for the time scale of protein unfolding at surfaces.[33] Of course, the spreading could be related to the density of the adsorbed layer, and the rate of these rearrangements should then depend on the crowding within the layer.[38]

For comparison to micelles that cannot spread, the adsorbed amount Γ vs $k_a ct$ is plotted for similarly sized star-block copolymers, as shown in Figure 4. In contrast to the copolymer micelles, the adsorption kinetics collapse to a single curve as a function of $k_a ct$, signifying that the adsorption rate is linear with concentration throughout the entire time frame. In the very least, this finding bolsters the argument that the nonoverlapping nature of the adsorption trajectories for the copolymer micelles could be the result of some spreading phenomenon. An interesting question that remains, nevertheless, is whether the adsorbed stars are themselves able to diffuse along the surface such that the layer can relax toward equilibrium. While a model that captures all relaxation events would be quite complicated, there are two signature details associated with so-called random sequential adsorption (RSA),[39] wherein adsorbed species are not permitted to diffuse laterally once adsorbed to the surface. Assuming that the star-block copolymers do not stick to one another on the surface and no relaxation events take place on the time scale of adsorption, the surface will eventually be coated with a layer whose distribution is determined by the deposition process. The maximum coverage that is achieved in this case, known as the jamming limit Γ_∞, is 54.7% of the density at closest packing, and the adsorption kinetics should approach this value with power-law behavior: $(\Gamma_\infty - \Gamma) \sim t^{-1/2}$.[40] Figure 5 shows the adsorbed amount of the star-block plotted against $t^{-1/2}$, which describes rather well the late-term behavior. It is expected that even a small amount of local translational freedom of the adsorbed species would dramatically alter RSA kinetics, enabling faster and denser adsorption. However, the data suggest self-diffusion of the adsorbed star-blocks is slow compared to the characteristic adsorption time. The extrapolated jamming limit is 1.67 mg/m^2, but unfortunately it is unclear which length scale would best define the "hard sphere" equivalent of the star-block to verify this value. From the extrapolated jamming limit, closest-packing coverage would occur at roughly 3 mg/m^2, which corresponds to an average radius of 60 nm per adsorbed star, which is not unreasonable The kinetics of star-block adsorption are therefore consistent with RSA adsorption, where each adsorbed molecule effectively blocks adsorption in an exclusion zone of ca. twice the diameter of the adsorbed molecule.

That being said, there are certain qualitative differences that emerge in comparing the adsorption of the star-blocks to the block copolymer micelles. The adsorption trajectories are compared in Figures 6 and 7, which show short-term and long-term behavior, respectively. Also plotted is the adsorption behavior of $NaPSS_{444}$ homopolymer, which has the same molecular weight as a single chain in the micelle. The homopolymer serves to further highlight differences between the micelles and the star-blocks.

First, the homopolymer and star-block show similar behavior with respect to the shape of their adsorption trajectories; nonetheless, the star-block reaches not only a higher adsorbed amount but also an apparent plateau surface coverage in less rescaled time than the homopolymer. The radius of a "hairy" micelle or star with f arms scales as $R_g = f^{1/5}N^{3/5}$.[41] On the

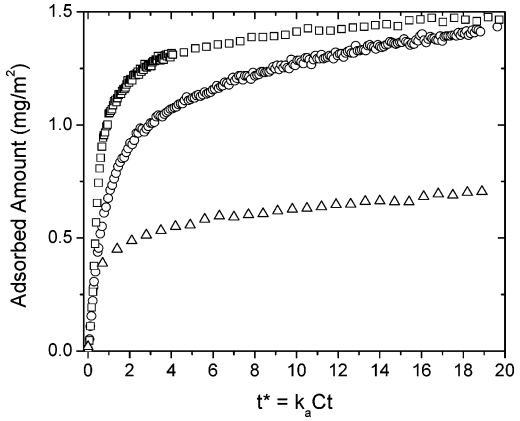

Figure 6. Adsorption of $PtBS_{15}$-*b*-$NaPSS_{438}$ (○), $NaPSS_{444}$ homopolymer (△), and $PtBS_{10}$-star-$NaPSS_{307}$ (□) to OTS at 0.3 M NaCl as a function of the rescaled time $k_a ct$.

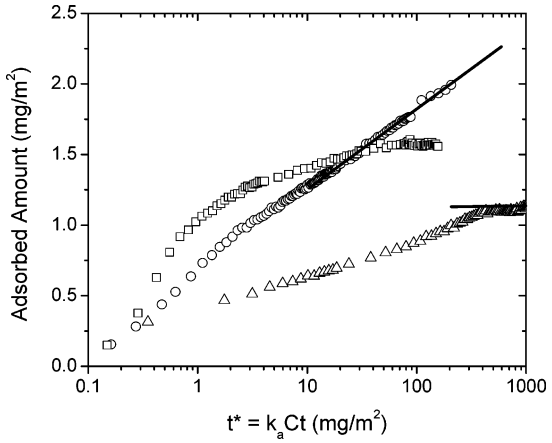

Figure 7. Adsorption of $PtBS_{15}$-*b*-$NaPSS_{438}$ (○), $NaPSS_{444}$ homopolymer (△), and $PtBS_{10}$-star-$NaPSS_{307}$ (□) to OTS at 0.3 M NaCl as a function of the rescaled time $k_a ct$.

other hand, the sum of the radii of the equivalent number of free chains is proportional to $fN^{3/5}$. Therefore, a star-block copolymer projects less surface area than the equivalent number of the chains that constitute its structure. This permits a higher adsorbed amount to be achieved before interactions between neighboring species interfere with the adsorption process. In the ensuing slow adsorption regime at long times, it is expected that the state of equilibrium should depend on the flexibility of the adsorbing species. As the number of arms increase, less interpenetration would be permitted between adsorbed species and saturation should be reached sooner. The more flexible the adsorbing species, the more opportunity it has to diffuse through a preformed layer and adopt a conformation that permits it to adsorb to the surface. Since diffusion through the preformed layer is subject to a large potential energy barrier, such systems are expected to equilibrate very slowly.

In contrast to both the star-block copolymer and the homopolymer systems, the adsorption trajectory of the diblock copolymer micelles follows fundamentally different behavior; this is especially apparent at long times in Figure 7. First, the decrease in the adsorption rate with increasing surface coverage is not as abrupt as observed in either the star-block or the homopolymer systems. For instance, while the adsorption rate of the block copolymer micelles drops more quickly from unity than that of the star-block copolymer, the transition is much more rounded. At an adsorbed amount of ~1.4 mg/m^2 (corresponding to a rescaled time of $t^* = 18$ mg/m^2), the adsorbed amount of the micelles surpasses the star-blocks and continues to increase with log(t) kinetics. Whereas both the homopolymer and the star-blocks reach an apparent plateau or saturation, the block copolymer micelles show no such behavior. Such a trend provides further indirect evidence that the block copolymer micelles are able to relax and reorganize during the adsorption process.

It has already been suggested that the block copolymer micelles initially adsorb through the attraction of the coronal arms to the surface. Once adsorbed, there must be some fast redistribution of the core blocks toward the surface followed by spreading to relieve local crowding within the micelle. As micelles begin to populate the surface, the adsorption rate slows in response to a reduction in available empty space. Given that the chains within an adsorbed micelle are still sufficiently mobile, it is expected that adsorbed NaPSS blocks will desorb from the surface in response to increasing surface coverage to alleviate the osmotic pressure in the layer near the surface. The more strongly adsorbed PtBS blocks, however, prevent complete desorption of the polymer. During this process, the adsorbed layer undergoes a continuous reorganization wherein the brush structure is formed, that is, where the PtBS blocks exclusively tether the soluble NaPSS blocks to the surface. The logarithmic growth regime is expected to persist until the osmotic pressure in the layer becomes sufficient to overcome the PtBS/OTS attraction.[14] If, on the other hand, relaxation and reorganization of the micelles could not occur on the time scale of the adsorption experiment, the adsorption of the block copolymer micelles would be expected to behave more in line with the star-blocks and approach a jamming limit.

IV. Conclusions

We have examined the implications of postadsorption rearrangements of PtBS-*b*-NaPSS diblock copolymer micelles on the adsorption kinetics to neutral surfaces. As a result of the core/shell structure of the micelle, micelles can adsorb if the coronal chains are sufficiently attractive to the surface. Structural development can still arise when both blocks adsorb, although the core blocks must possess a stronger affinity for the surface. These conditions, unfortunately, also create circumstances conducive to long-lived transient states and history-dependent adsorption. Nonetheless, the mobility of polymers at surfaces is not thoroughly understood, and kinetic experiments can lead to a more thorough appreciation of the interplay between kinetic and thermodynamic issues in governing the adsorbed layer structure. More universally, these findings demonstrate that the adsorption of associating polymers can display complex behavior, wherein not only does the topology of the adsorbing species play a critical role but also relaxation events in the adsorbed layer.

Acknowledgment. This work was supported by the NIRT and MRSEC Program of the National Science Foundation under Awards CTS-0103516 and DMR-0080034.

References and Notes

(1) Tassin, J. F.; Siemens, R. L.; Tang, W. T.; Hadziioannou, G.; Swalen, J. D.; Smith, B. A. *J. Phys. Chem.* **1989**, *93*, 2106−2111.
(2) Amiel, C.; Sikka, M.; Schneider, J. W.; Tsao, Y. H.; Tirrell, M.; Mays, J. W. *Macromolecules* **1995**, *28*, 3125−3134.
(3) Tirrell, M.; Parsonage, E.; Watanabe, H.; Dhoot, S. *Polym. J.* **1991**, *23*, 641−649.
(4) Motschmann, H.; Stamm, M.; Toprakcioglu, C. *Macromolecules* **1991**, *24*, 3681−3688.
(5) Abraham, T.; Giasson, S.; Gohy, J. F.; Jerome, R.; Muller, B.; Stamm, M. *Macromolecules* **2000**, *33*, 6051−6059.
(6) Styrkas, D. A.; Butun, V.; Lu, J. R.; Keddie, J. L.; Armes, S. P. *Langmuir* **2000**, *16*, 5980−5986.

(7) De Cupere, V. M.; Gohy, J.-F.; Jerome, R.; Rouxhet, P. G. *J. Colloid Interface Sci.* **2004**, *217*, 60−68.
(8) Hamley, I. W.; Conell, S. D.; Collins, S. *Macromolecules* **2004**, *37*, 5337−5351.
(9) Munch, M. R.; Gast, A. P. *Macromolecules* **1988**, *21*, 1366−1372.
(10) Munch, M. R.; Gast, A. P. *J. Chem. Soc., Faraday Trans.* **1990**, *86*, 1341−1348.
(11) Alexander, S. *J. Phys. (Paris)* **1977**, *38*, 983−987.
(12) Dan, N.; Tirrell, M. *Macromolecules* **1993**, *26*, 4310−4315.
(13) Johner, A.; Joanny, J. F.; Marques, C. *Physica A* **1991**, *172*, 285−289.
(14) Johner, A.; Joanny, J. F. *Macromolecules* **1990**, *23*, 5299−5311.
(15) Halperin, A.; Tirrell, M.; Lodge, T. *Adv. Polym. Sci.* **1992**, *100*, 31−71.
(16) Israels, R.; Leermakers, F. A. M.; Fleer, G. J. *Macromolecules* **1995**, *28*, 1626−1634.
(17) Israels, R.; Scheutjens, J.; Fleer, G. J. *Macromolecules* **1993**, *26*, 5405−5413.
(18) Wittmer, J.; Joanny, J. F. *Macromolecules* **1993**, *26*, 2691−2697.
(19) Argillier, J. F.; Tirrell, M. *Theor. Chim. Acta* **1992**, *82*, 343−350.
(20) Schneider, H. M.; Frantz, P.; Granick, S. *Langmuir* **1996**, *12*, 994−996.
(21) van Eijk, M. C. P.; Cohen Stuart, M. A. *Langmuir* **1997**, *13*, 5447−5450.
(22) Schaaf, P.; Talbot, J. *J. Chem. Phys.* **1989**, *91*, 4401−4409.
(23) Dijt, J. C.; Cohen Stuart, M. A.; Hofman, J. E.; Fleer, G. J. *Colloids Surf.* **1990**, *51*, 141−158.
(24) Yang, J. C.; Mays, J. W. *Macromolecules* **2002**, *35*, 3433−3438.
(25) Valint, P. L.; Bock, J. *Macromolecules* **1988**, *21*, 175−179.
(26) Jasperson, S.; Schnatterly, S. *Rev. Sci. Instrum.* **1969**, *40*, 761.
(27) Azzam, R. M.; Bashara, N. M. *Ellipsometry and Polarized Light*; North-Holland Publication: Amsterdam, 1979.
(28) Toomey, R.; Mays, J.; Tirrell, M. *Macromolecules* **2004**, *37*, 905−911.
(29) Zhang, Y. Y. Ph.D. Thesis, University of Minnesota, 1996.
(30) Toomey, R. G.; Mays, J.; Holley, W.; Tirrell, M. *Macromolecules* **2005**, *38*, 5137−5143.
(31) Santore, M. In *Colloid-Polymer Interactions: From Fundamentals to Practice*; Farinato, R. S., Dubin, P. L., Eds.; John Wiley & Sons: New York, 1999; pp 127−145.
(32) Calonder, C.; van Tassel, P. R. *Langmuir* **2001**, *17*, 4392−4395.
(33) van Eijk, M. C. P.; Cohen Stuart, M. A. *Langmuir* **1997**, *13*, 5447−5450.
(34) van Eijk, M. C. P.; Cohen Stuart, M. A.; Rovillard, S.; De Conink, J. *Eur. Phys. J. B* **1998**, *1*, 233−244.
(35) van Tassel, P. R.; Guemouri, L.; Ramsden, J. J.; Tarjus, G.; Viot, P.; Talbot, J. *J. Colloid Interface Sci.* **1998**, *207*, 317−323.
(36) Calonder, C.; van Tassel, P. R. *Langmuir* **2001**, *17*, 4392−4395.
(37) Ligoure, C. *Macromolecules* **1991**, *24*, 2968−2972.
(38) Zhao, J.; Granick, S. *J. Am. Chem. Soc.* **2004**, *126*, 6242−6243.
(39) Talbot, J.; Tarjus, G.; van Tassel, P. R.; Viot, P. *Colloids Surf., A* **2000**, *165*, 287−324.
(40) Ramsden, J. J. *Phys. Rev. Lett.* **1993**, *71*, 295−298.
(41) Daoud, M.; Cotton, J. P. *J. Phys. (Paris)* **1982**, *43*, 531−538.

MA051097I